Hinfp is a guardian of the somatic genome by repressing transposable elements

Niraj K. Nirala[a], Qi Li[a], Prachi N. Ghule[b,c], Hsi-Ju Chen[a], Rui Li[d], Lihua Julie Zhu[a,d], Ruijia Wang[a], Nicholas P. Rice[a], Junhao Mao[d], Janet L. Stein[b,c], Gary S. Stein[b,c], Andre J. van Wijnen[e,f], and Y. Tony Ip[a,1]

[a]Program in Molecular Medicine, University of Massachusetts Medical School, Worcester, MA 01605; [b]Department of Biochemistry, University of Vermont College of Medicine, Burlington, VT 05405; [c]University of Vermont Cancer Center, University of Vermont College of Medicine, Burlington, VT 05405; [d]Department of Molecular, Cell, and Cancer Biology, University of Massachusetts Medical School, Worcester, MA 01605; [e]Department of Orthopedic Surgery, Mayo Clinic, Rochester, MN 55905; and [f]Department of Biochemistry and Molecular Biology, Mayo Clinic, Rochester, MN 55905

Edited by Hugo Bellen, Baylor College of Medicine, Houston, TX, and approved September 3, 2021 (received for review January 14, 2021)

Germ cells possess the Piwi-interacting RNA pathway to repress transposable elements and maintain genome stability across generations. Transposable element mobilization in somatic cells does not affect future generations, but nonetheless can lead to pathological outcomes in host tissues. We show here that loss of function of the conserved zinc-finger transcription factor Hinfp causes dysregulation of many host genes and derepression of most transposable elements. There is also substantial DNA damage in somatic tissues of *Drosophila* after loss of Hinfp. Interference of transposable element mobilization by reverse-transcriptase inhibitors can suppress some of the DNA damage phenotypes. The key cell-autonomous target of *Hinfp* in this process is *Histone1*, which encodes linker histones essential for higher-order chromatin assembly. Transgenic expression of Hinfp or Histone1, but not Histone4 of core nucleosome, is sufficient to rescue the defects in repressing transposable elements and host genes. Loss of Hinfp enhances Ras-induced tissue growth and aging-related phenotypes. Therefore, Hinfp is a physiological regulator of Histone1-dependent silencing of most transposable elements, as well as many host genes, and serves as a venue for studying genome instability, cancer progression, neurodegeneration, and aging.

Drosophila | genome stability | Hinfp | somatic | transposable elements

Complex genomes like those of humans require elaborate mechanisms to maintain stability throughout lifespans and otherwise will lead to developmental problems and diseases (1–3). Large portions of eukaryotic genomes contain repetitive elements that include tandem repeats such as the Alu family and transposable elements (TEs) such as LINE-1, and these two elements alone make up 20% of human DNA (4, 5). TEs can be mobilized to generate new integrations in the host genome, therefore affecting genome function, stability, and evolution (2, 6, 7). TE jumping in germ cells may cause developmental defects of individual offspring, but nonetheless may benefit genome evolution for the following generations and therefore long-term fitness of the species (1, 2, 7). In somatic cells, uncontrolled TE expression offers no obvious benefits, because new insertional changes do not get passed on to future generations, but instead can lead to pathological outcomes (3, 8–12).

Germ cells possess the Piwi-interacting RNA (piRNA) pathway to repress TEs to maintain genome stability across generations (13–15). piRNA transcribed from clusters of remnant TE sequences in genomes interact with Argonaute proteins such as Piwi to form a complex that guides the degradation of target RNA from corresponding TEs (8, 14–16). In somatic cells, loss of function of piRNA pathway, even together with the short interfering (siRNA) pathway, however, causes only a mild increase of TE expression (17–21), suggesting that other components may play important roles in TE repression in somatic tissues.

Epigenetic components, including DNA methylation, chromatin proteins, and their modification factors, are frequently used to control genome stability (2, 6). In germ cells, the piRNA pathway has been shown to not only degrade TE transcripts, but also collaborate with chromatin regulatory factors to reduce TE expression at the transcription level (16, 22–25). In somatic cells, because of a lesser involvement of piRNA and siRNA pathways (12, 17, 19–21), epigenetic components may play even more important roles in TE silencing. TE sequences have much higher density in centromeres and telomeres, where heterochromatin structure is commonly involved in gene silencing (2, 6). Even in euchromatic regions where many TEs are present, local heterochromatin formation is probably involved to repress TE expression (23, 26–29). The mechanism of selective heterochromatin formation associated with TEs and the relaxation of such a mechanism may shed light on somatic genome instability and disease progression.

In this report, we demonstrate that the zinc-finger transcriptional regulator Histone Nuclear Factor P (Hinfp) is critical for regulating many *Drosophila* host genes and silencing of most TEs in somatic tissues of *Drosophila*. Hinfp silences TEs through maintaining the expression of Histone1, which normally functions as the linker histone for higher-order chromatin assembly and gene repression. The loss of Hinfp enhances cancer- and aging-related phenotypes, suggesting that Hinfp is a guardian of somatic genomes and a venue for studying diseases related to genome instability.

Results

Hinfp Is Essential for Optimal Development, but Not Tissue Patterning. The *Drosophila* adult midgut epithelium contains stem cells and their progenies, including enterocytes (ECs) for nutrient absorption

Significance

Repression of the large number of transposable elements in eukaryotic genomes is essential for genome stability. The Piwi-interacting RNA and short interfering RNA pathways are critical for repressing transposable elements in germlines, but the repression of transposable elements in somatic tissues involves other components. While the mammalian Hinfp has been shown to regulate Histone4 and cell-cycle progression, our manuscript provides evidence that a function of the *Drosophila* Hinfp is to maintain Histone1 expression to repress most transposable elements in somatic genomes. This Hinfp–Histone1 axis provides a venue to study maintenance of genome stability and progression of pathological outcomes.

Author contributions: N.K.N., J.M., J.L.S., G.S.S., A.J.v.W., and Y.T.I. designed research; N.K.N., Q.L., P.N.G., H.-J.C., and Y.T.I. performed research; N.K.N., Q.L., P.N.G., H.-J.C., R.L., L.J.Z., R.W., N.P.R., J.M., J.L.S., G.S.S., A.J.v.W., and Y.T.I. analyzed data; and N.K.N., R.L., L.J.Z., R.W., J.L.S., G.S.S., A.J.v.W., and Y.T.I. wrote the paper.

The authors declare no competing interest.

This article is a PNAS Direct Submission.

[1]To whom correspondence may be addressed. Email: Tony.Ip@umassmed.edu.

This article contains supporting information online at https://www.pnas.org/lookup/suppl/doi:10.1073/pnas.2100839118/-/DCSupplemental.

Published October 7, 2021.

and enteroendocrine cells (EEs) for hormone secretion (30, 31). This epithelium has a high rate of cell turnover and represents an active tissue that involves stem-cell-supported tissue homeostasis (32, 33). During our ongoing RNA interference (RNAi) screens to investigate genes that are involved in the adult *Drosophila* midgut homeostasis, we observed that loss of function of the gene CG17829 by RNAi caused a decreased stem cell proliferation (Fig. 1 *C–E*). CG17829 is homologous to mammalian HINFP (Fig. 1*A*), which is a zinc-finger nuclear factor that binds a highly conserved element in the *Histone4* (*His4*) gene promoter and positively regulates *His4* expression required for cell-cycle progression (34–37). The *Drosophila* CG17829/*Hinfp* gene is located on the X chromosome (38). We generated two independent deletion alleles of *Hinfp* by using CRISPR-mediated genome engineering, as well as obtained a previously generated ethyl methanesulfonate (EMS)-induced point mutant (38) (Fig. 1 *A* and *B*). The *Hinfp*$^{-}$/*Y* mutant male animals developed to become pupae, but died before eclosion as adults (*SI Appendix*, Fig. S1*A*). These mutant pupae had largely normal development (Fig. 1 *F* and *G*), and pharate adults pulled out of the pupal cases had limb movements, but died soon after. Maternal levels of *Hinfp* RNA are high (FlyBase), which may mask early zygotic developmental requirements for Hinfp. Nonetheless, mutant larval midguts (Fig. 1*H*) and pupal testes (Fig. 1 *I–P*) had reduced proliferation. Moreover, mutant pupal midguts showed abnormal morphology, especially in posterior regions (Fig. 1 *Q* and *R*), and staining for Heterochromatin Protein 1 (HP1) showed a multifoci pattern in the nuclei of mutant midgut cells (Fig. 1 *S* and *T*). Overall, loss of *Hinfp* leads to pupal lethality with largely normal development, but defects in proliferation and chromatin structure.

RNA Expression Profiling Reveals Derepression of Most TEs after Loss of Hinfp. Transgenic expression of an hemagglutinin (HA)-tagged Hinfp revealed that it is a nuclear protein (*SI Appendix*, Fig. S1 *B* and *C*), consistent with a function in transcription. To examine possible gene-expression defects, we performed deep sequencing of gut RNA isolated from *Hinfp* mutant pupae. Over 1,000 *Drosophila* genes (~10% of all genes) showed significant change of expression (Fig. 2*A*) (Gene Expression Omnibus [GEO] accession no. GSE138430), including reduced expression of many *Histone* genes as expected (*SI Appendix*, Table S1) (FigShare, https://doi.org/10.6084/m9.figshare.15506415.v1). Surprisingly, there were even more up-regulated genes in the mutant (Fig. 2*A*), and smaller transcripts showed greater increases of expression (*SI Appendix*, Fig. S2 *A* and *A'*). Moreover, Gene Ontology analysis suggested defects in processes such as replication, mitochondrial function, and transposition (*SI Appendix*, Fig. S3 *A* and *B*). The derepression of many small genes and misregulation of transposition prompted us to examine TE expression in addition to *Drosophila* genes. The result revealed that 96/155 (62%) of TE families had significantly increased expression, while only very few TE families had slightly decreased expression (Fig. 2*B* and *SI Appendix*, Fig. S2*B*). The increase varied from 2-fold to over 100-fold and included LTR and LINE and some DNA elements such as transib1-3 in the TIM family (Fig. 2 *B* and *C* and *SI Appendix*, Fig. S2*B*). qPCR confirmed substantially increased RNA expression of many of these TEs in pupal guts (Fig. 2*D*). The derepression of TEs occurred in as early as third-instar larval stage, while first-instar mutant larvae had normal TE expression (*SI Appendix*, Fig. S2 *C* and *D*).

Hinfp Mutant Tissues Have Increased DNA Damage and Loss of His1 Expression. Increased expression of TEs can cause genome instability in host tissues (3, 6). We used antibody to stain for γH2Av, which is the phosphorylated H2A variant that associates with regions of DNA damage (6, 39). The midguts and Malpighian tubules from mutant pupae had clearly increased γH2Av staining in almost all cells (Fig. 3 *A–D*). We isolated genomic DNA from pupal midguts, and native agarose gel analysis confirmed that there was a substantial increase of smaller-sized DNA, suggesting physical DNA double-strand breaks (Fig. 3*E*). The increase of γH2Av staining was also observed in third-instar larval midgut (Fig. 3 *F* and *G*), salivary gland (Fig. 3 *H* and *I*), fat body, imaginal discs, and many brain cells, as well as in adult mutant clones and RNAi cells (see below). These results together demonstrate that DNA damage can happen in most somatic genomes.

We investigated the underlying mechanism for the extensive TE derepression and DNA damage after loss of *Hinfp*. Previous publications have shown that the piRNA and siRNA pathways contribute to repression of somatic TEs, but the phenotypes appear to be much less severe than we show here in the *Hinfp* mutants (13, 17–21, 23). Moreover, based on our RNA-sequencing (RNAseq) results, there was no apparent loss of expression of these pathways in the *Hinfp* mutants because the RNA levels of *Su(var)3-9*, *Dicer-1*, and *Dicer-2* did not change, and the levels of *piwi*, *Argonaute2*, *Argonaute3*, *aubergine*, and *maelstrom* were up-regulated (*SI Appendix*, Fig. S4*A*), which may indicate instead a reaction to increased TE expression. Therefore, we surmised that there should be another primary defect responsible for the TE derepression in the *Hinfp* mutants. When examining the expression of *Histone* genes by qPCR, we noticed that the core *Histone* genes (*His2A*, *His2B*, *His3*, and *His4*) exhibited the expected decreases, of ~50%, but the linker *Histone* gene *His1* surprisingly exhibited more than 95% decrease (Fig. 3 *J–N*). The *Drosophila Histone* gene complex encompasses over 100 *Histone* genes arranged as 23 repeats of the 5 *Histone* genes in the order of *His1*, *His2A*, *His2B*, *His4*, and *His3* (40–42). Previous studies have shown that knockdown of *His1* expression by RNAi in *Drosophila* and mammalian tissues results in various chromosome defects and derepression of TEs (43–51) and, therefore, may well explain our observed phenotypes. We used an antibody that could detect all expressed His1 proteins and showed that the overall expression in *Hinfp* mutants decreased to almost undetectable levels based on Western blotting of gut extracts and tissue staining of gut cells (Fig. 3 *O–Q*). Similar loss of His1 expression was confirmed in mutant larval midguts by qPCR and Western blots (*SI Appendix*, Fig. S4 *B–F*), as well as by tissue staining in multiple larval and pupal tissues (Fig. 4 and *SI Appendix*, Fig. S4 *G–N*).

Loss of His1 Tightly Correlates with DNA Damage. We observed a tight correlation between loss of His1 and increase of γH2Av staining in multiple cells and tissues of *Hinfp* mutants. As described above, many tissues examined in addition to pupal guts also showed loss of His1 with increased γH2Av staining, including larval midgut, larval wing disk (Fig. 4 *A–H*), larval fat body, larval salivary gland, and pupal testis (*SI Appendix*, Fig. S4 *I–N*). This loss of His1 in *Hinfp* mutants, however, is not universal in all cells; for example, testis tip cells still showed some His1 staining (*SI Appendix*, Fig. S4 *M* and *N*, arrows). A more interesting exception was revealed by comparison of two layers of cells within the same pupal midgut, such that mutant epithelial cell nuclei had lost His1 expression and increased γH2Av staining (Fig. 4 *I–L*), while the neighboring layer of visceral muscle cell nuclei showed retention of His1 expression and no increase of γH2Av staining (Fig. 4 *M–P*). Another example is the larval brain ventral nerve cord, where many large nuclei (probably neuroblasts) lost His1 signal in the mutant and also had increased γH2Av staining (Fig. 4 *Q–U*, arrows). We note that double staining of His1 and γH2Av is technically not possible because the antibodies are both mouse monoclonals, and, therefore, the location of these staining in the ventral nerve cord was based on characteristic patterns along the midline. Overall, most *Hinfp* mutant tissues and cells have lost their His1 expression together with increased γH2Av staining. Wherever there is remnant His1, there is no increased γH2Av staining.

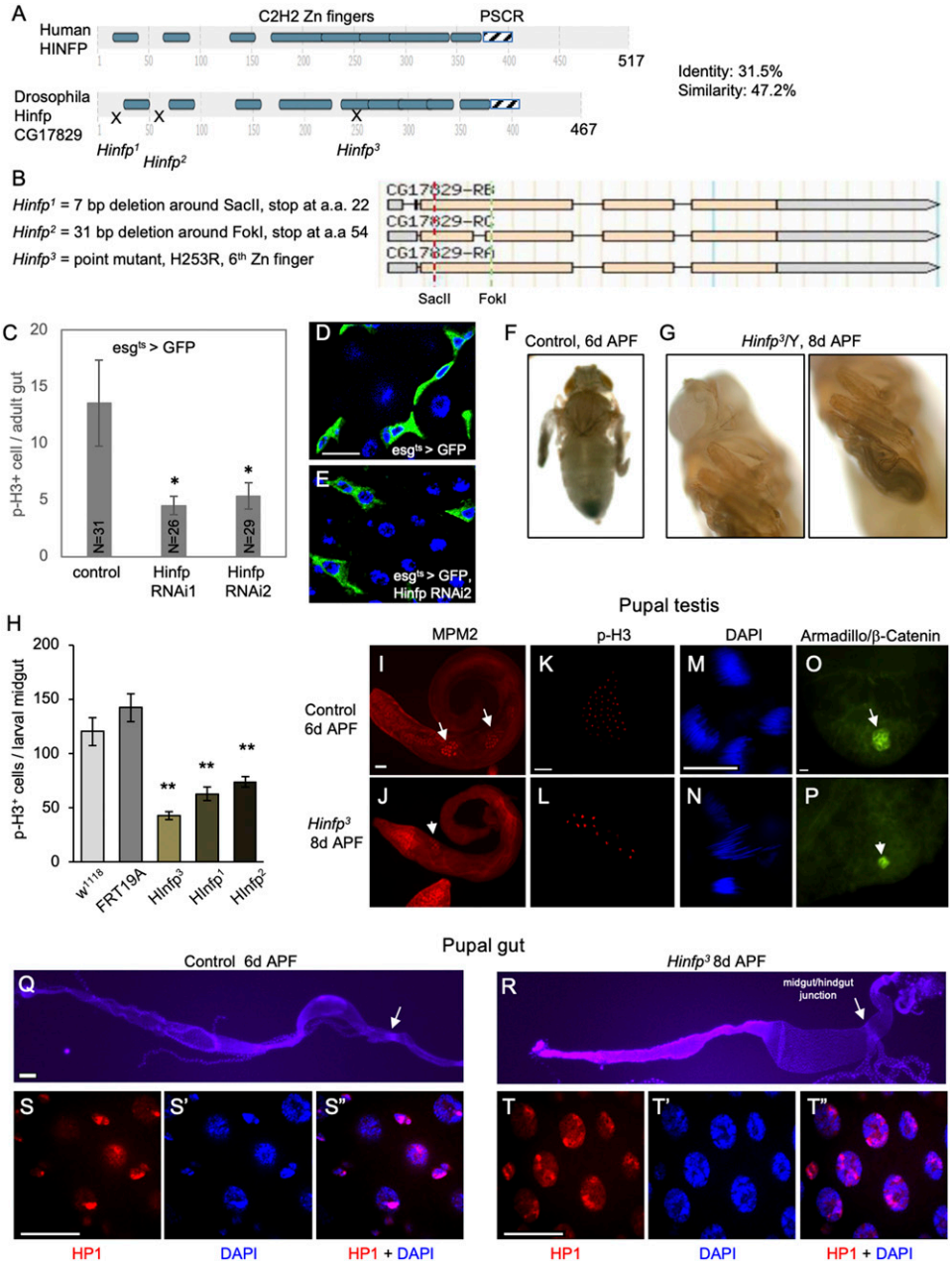

Fig. 1. Hinfp is essential for optimal development, but not tissue patterning. (*A*) The primary structures of human HINFP and *Drosophila* Hinfp proteins both contain nine C2H2-type zinc fingers and the HINFP-specific conserved region (PSCR) essential for DNA binding (35). The locations of the mutations are shown as ×. (*B*) The *Drosophila Hinfp* locus encodes three splice isoforms (FlyBase). Two deletion alleles $Hinfp^1$ and $Hinfp^2$ were generated in our laboratory by CRISPR–guide RNAs targeting sequences near the SacII and FokI restriction sites, while $Hinfp^3$ was an EMS-induced point mutation from a previous report (38). (*C*–*E*) The two transgenic UAS–Hinfp dsRNA construct containing fly lines (Hinfp RNAi) were crossed with the esg–Gal4, tub–Gal80^{ts}, UAS–CD8GFP (esg^{ts}> GFP) driver line. RNAi1 is v110592 and RNAi2 is v41659. Adult flies obtained from the crosses were aged for 7 to 10 d at room temperature, ~23 °C, and then incubated at 29 °C for 6 d. Guts were dissected and used for immunostaining using the antiphosphorylated-Histone3 (p-H3) antibody as a mitotic marker. The positive p-H3 staining was counted throughout the whole midgut, and the average is plotted, as shown in *A*. The error bar is SEM. $*P < 0.05$ (Student's *t* test). *D* and *E* show representative confocal images of control and Hinfp RNAi guts. The nuclear DNA is revealed by DAPI staining (blue), and the cytoplasmic and membrane CD8–GFP signal (green) outlines the precursor cells, including ISCs and EBs. Scale bar in *D*: 20 um. (*F* and *G*) Photos of pharate adults around eclosion. Control animals eclose around 6 d after puparium formation (6d APF) at 23 °C. Most *Hinfp* mutant males did not eclose after 8 d, but still showed normal developmental morphology. (*H*) A graph showing proliferation defects in *Hinfp* mutant larval midguts. Third-instar larval guts were used for phosphorylated Histone3 (p-H3) antibody staining as a mitotic marker for the adult midgut precursor (AMP) division. $**P < 0.01$ ($n = 35$). Control strains were w^{1118} and FRT19A, which is the parental for generation of the mutants. (*I*–*P*) Images of wild-type and mutant pupal testes, showing mutants had abnormal morphology, especially at the anterior tip (left, *I* and *J*), fewer mitotic/meiotic clusters (arrows in *I* and *J*), disorganized mitotic/meiotic clusters with fewer p-H3–stained nuclei (*K* and *L*), disorganized spermatid head DNA staining (*M* and *N*), and a smaller stem cell cluster at the anterior tip of testis revealed by β-catenin staining (arrows in *O* and *P*). Scale bar in *I*: 100 um. Scale bar in *K*, *M*, and *O*: 20 um. (*Q* and *R*) Light microscopic images of DAPI-stained pupal guts, with anterior to the left. The mutant guts have overall shorter length, and the posterior midguts are incompletely extended (*R*, left of the arrow indicating midgut/hindgut junction). (Scale bar in *Q*: 100 μm.) (*S* and *T*) High-magnification confocal images showing the mutant midgut cells have disorganized chromatin structure, as revealed by immunofluorescence staining for HP1 (red). DAPI staining is blue. (Scale bar in *S*, *T*: 20 μm.)

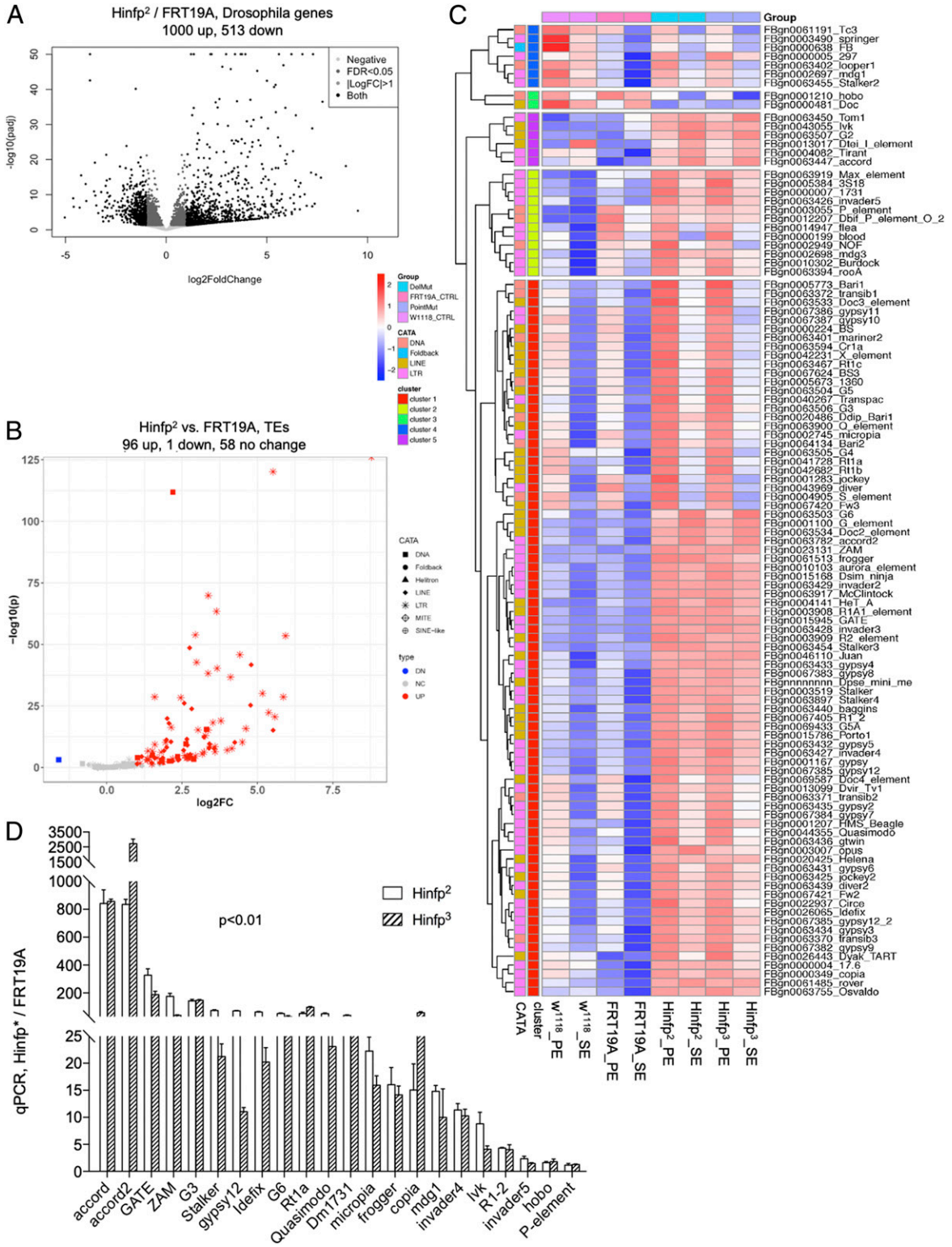

Fig. 2. RNA expression profiling reveals derepression of TEs after loss of Hinfp. (*A*) Volcano plot showing relative expression of *Drosophila* genes based on whole-transcriptome sequencing of pupal gut RNA from 50 guts of each genotype. Four independent mutant and control samples were sequenced, and a representative plot based on *Hinfp²* vs. FRT19A pair-ended sequencing is shown. (*B*) Volcano plot showing relative expression of TE families in *Hinfp²* pupal guts comparing to FRT19A, based on pair-ended sequencing of the two samples. (*C*) Heatmap of TE sequences analyzed with RNAseq data. The map represents results of *Hinfp²* and *Hinfp³* compared with control w^{1118} or FRT19A strains, with each sequenced as single-ended (SE) or pair-ended (PE). The relative expression of each TE RNA sequence in all eight samples was calculated as a Z-score and represented from low/blue (−2) to high/red (+2). (*D*) Quantification of RNA expression of representative TEs by RT-PCR. The PCR expression level of *ribosomal protein 49 (rp49)* in parallel was used to normalize the expression of each TE sequence for each experiment and set as one for control samples and plotted as fold change for each TE in the mutants. The value is the average of four independent PCRs. Error bar is SEM, and all samples have $P < 0.01$, based on Student's *t* test, except that the last two TEs had no significant change.

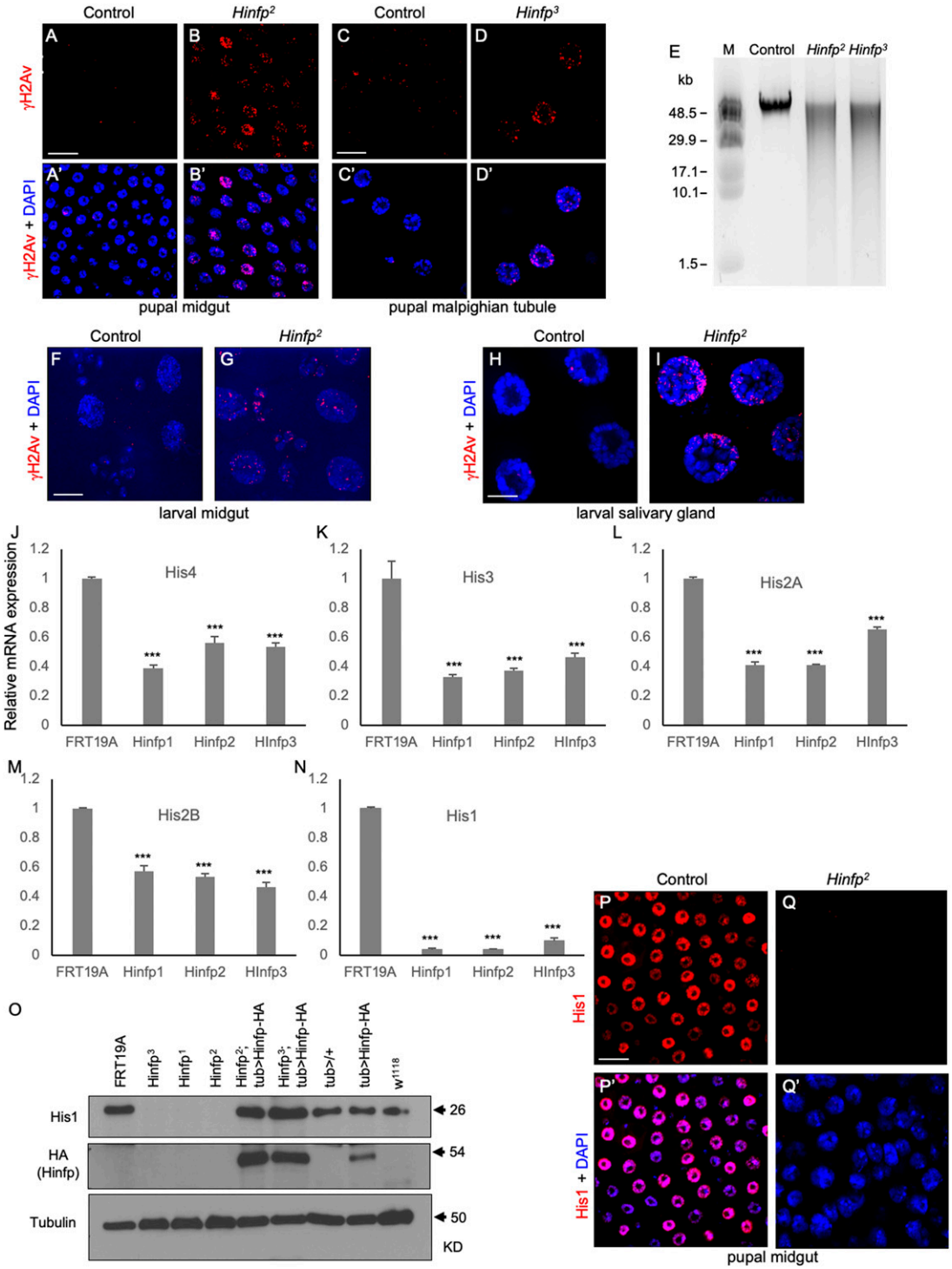

Fig. 3. Hinfp mutant tissues have increased DNA damage and loss of His1 expression. (*A–D*) Confocal images of immunofluorescence staining of pupal midguts and Malpighian tubules using the γH2Av antibody that recognizes the phosphorylated H2Av, which is associated with damaged DNA. *A′–D′* are images double-labeled with γH2Av in red and DAPI in blue. (Scale bars: 20 μm [*A* and *C*].) Control was FRT19A. (*E*) Image of native agarose gel electrophoresis separation of genomic DNA isolated from 40 pupal guts each of the indicated genotypes. Lane M is the DNA molecular marker in kilobase pairs. (*F–I*) Confocal images showing double staining of γH2Av in red and DAPI in blue. The tissues were larval midgut and salivary gland. (Scale bars: 20 μm.) (*J–N*) qPCR analysis of the indicated *Histone* gene RNA expression using total RNA isolated from 30 pupal guts. The expression level of each gene is normalized with parallel *rp49* qPCR as internal control and set as one for FRT19A samples. The expression levels in the three mutants were plotted as fraction of control. Error bar is SEM. ***$P < 0.001$. (*O*) Western blot analysis of His1 protein expression in pupal gut extracts. The genotype of flies used for gut-extract preparation is as indicated to the top of each lane. The antibody used for the blots are as indicated to the left. The antibody for His1 recognized all *Drosophila* His1 proteins. Tubulin was used as a loading control for each sample. The transgenic UAS construct contained the HA tag sequence and was used as the epitope for assessing transgenic expression of the UAS–Hinfp–HA, driven by tubulin–Gal4 (tub>). (*P* and *Q*) Confocal images of pupal midgut immunofluorescence staining for His1 protein. The *P′* and *Q′* panels are images double-labeled with His1 in red and DAPI in blue. Scale bar in *P*: 20 um.

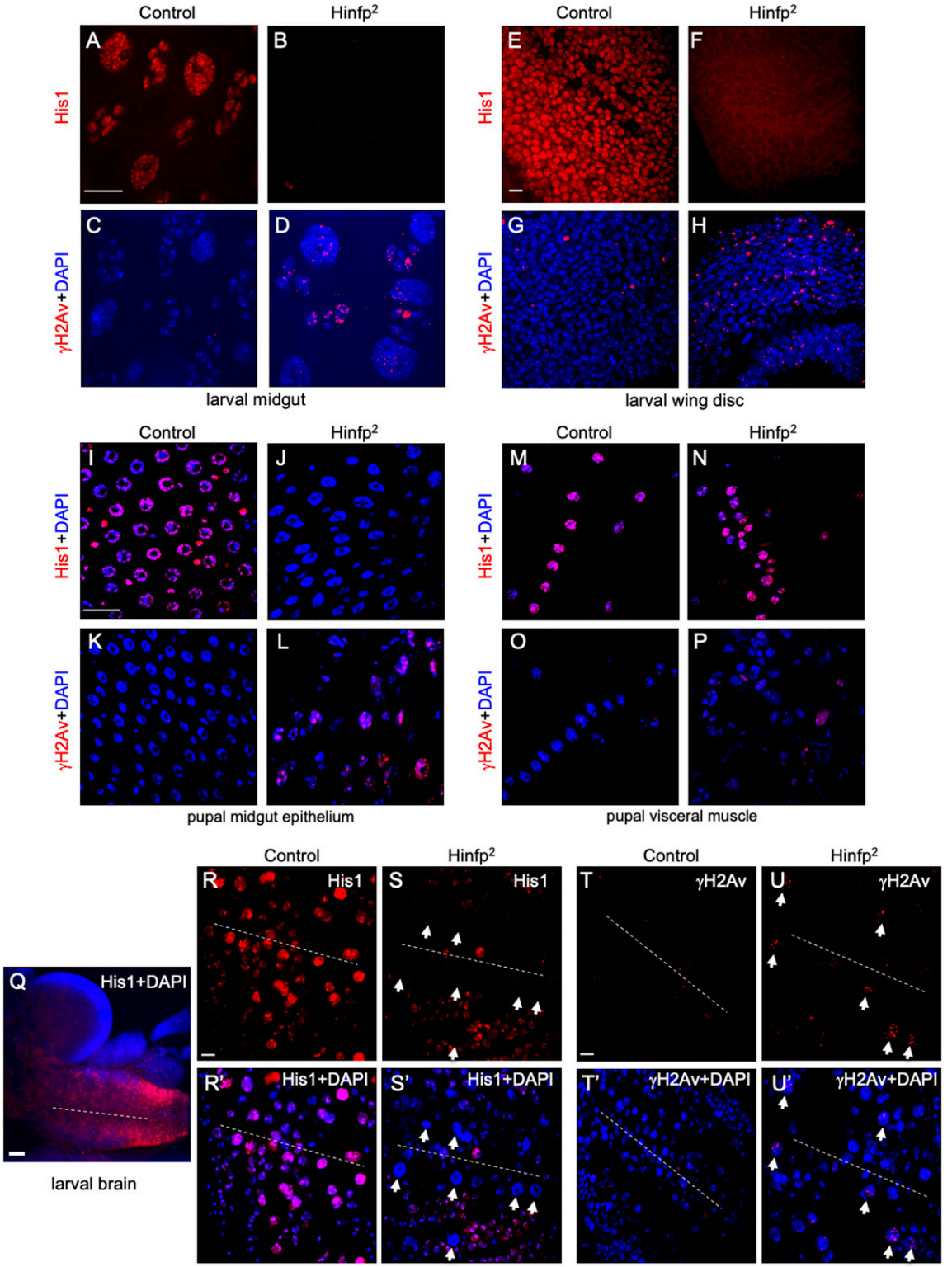

Fig. 4. Loss of His1 tightly correlates with DNA damage. (*A–D*) Confocal images showing His1 and γH2Av staining in third-instar larval midguts. The big nuclei are larval ECs, and the small cell clusters are adult midgut precursors (AMPs). All the cells showed loss of His1 staining and increased γH2Av staining in *Hinfp* mutants. Scale bar in *A*: 20 um. (*E–H*) Confocal images showing His1 and γH2Av staining in larval wing discs. In *Hinfp* mutants, His1 staining largely disappeared from all disk cells, and many disk cells had increased staining for γH2Av. Scale bar in *E*: 20 um. (*I–L*) Confocal images showing His1 and γH2Av staining in pupal midgut epithelia. The tissues from *Hinfp* mutant showed loss of His1 staining and increased γH2Av staining. Scale bar in *I*: 20 um. (*M–P*) Confocal images showing His1 and γH2Av staining in the adjacent layers of muscle nuclei in the same pupal midgut as *I–L*, respectively. Many muscle nuclei retained good His1 staining and showed much less γH2Av staining in *Hinfp* mutants. (*Q–U*) *Q* shows a low magnification of a WT third-instar larval brain and ventral nerve cord, with the white dash-line representing the ventral midline. Scale bar in *Q*: 100 um. *R* shows higher magnification of His1 staining in both big and small nuclei around the ventral midline. In *Hinfp* mutants, the His1 staining was absent in many big nuclei that probably were neuroblasts (*S*, arrows). Similar big nuclei in parallel experiments were the ones that contained the most consistent increase of γH2Av staining (*U*, arrows). Scale bar in *R*, *T*: 20 um.

Regulation of His1 Expression, TE Repression, and Genome Integrity by Hinfp Is Cell-Autonomous. To further determine if the requirement of Hinfp in maintaining His1 expression, TE silencing, and genome integrity is cell-autonomous, we performed a series of cell-specific RNAi and mutant clonal experiments. We used the *escargot* promoter-driven Gal4 system (abbreviated as esg^{ts}>) to direct upstream activation sequence (UAS)-dependent transgenic expression in adult midgut precursor cell nests that include intestinal stem cells (ISCs) and enteroblasts (EBs), but not in mature ECs. The system also included a temperature-sensitive repressor Gal80^{ts} to permit Gal4-activated expression when the incubation temperature was raised to 29 °C and a UAS-driven GFP for cell marking. Knockdown of *Hinfp* by using two different UAS–*Hinfp* double-stranded RNA (dsRNA) transgenic constructs via this esg^{ts}> system was sufficient to cause loss of His1 expression (Fig. 5 *A* and *B*, arrows) concomitant with strong γH2Av staining (Fig. 5 *C* and *D*), specifically in ISCs/EBs that were marked by GFP. Next, we used the mosaic analysis with a repressible cell marker (MARCM) technique to induce mitotic recombination in heterozygous female flies to produce GFP-marked homozygous *Hinfp*$^{-/-}$ mutant clones, each originated from a single mitotic ISC (31, 52–54). In adult midguts, these GFP+ mutant clones showed a clear loss of His1 at 10 d after clone induction (Fig. 5 *E* and *G*). These MARCM mutant clones showed noticeable overgrowth in the middle midgut regions and after more than 10 d (*SI Appendix*, Fig. S5). However, this overgrowth phenotype is variable along different regions of the gut and at different times and may represent complex secondary reactions to the genome instability over time. The adult female follicle cells that encircle the developing egg chamber are also somatic, and follicle-cell MARCM mutant clones also lost their His1 staining (Fig. 5*I*). In both gut and follicle epithelia, increased γH2AV staining was evident for these GFP+ mutant clones (Fig. 5 *F*, *H*, and *J*). To quantify TE expression, we subjected adult flies to multiple heat shocks and let them recover for 10 d to generate more mutant clones and then used whole guts for RNA isolation. The RNA samples isolated from guts that contained *Hinfp* mutant clones had significantly higher TE expression compared to those that contained FRT19A control clones (Fig. 5*K*). Therefore, loss of His1, derepression of TEs, and DNA damage all coincide with loss of Hinfp function.

His1 Functions Downstream of Hinfp to Repress TEs and Maintain Genome Integrity. We next performed a series of transgenic rescue experiments to assess whether His1 is functionally important for the downstream defects of *Hinfp* mutations. We crossed two different *Hinfp* mutant flies with transgenic flies harboring HA-epitope-tagged UAS–complementary DNA (cDNA) vectors for *Hinfp*, *His1*, *His4*, or an unrelated kinase, *misshapen* (*msn*). Strikingly, transgenic expression of Hinfp or its putative target His1 restored the viability of mutant pupae to become adult flies. In contrast, expression of His4 or Msn did not rescue the viability (Fig. 6*A*). As anticipated, His1 expression was largely rescued by expression of Hinfp based on Western blotting (Fig. 3*O*) and tissue staining (Fig. 6 *B*–*E*). Staining of γH2Av was also returned to an undetectable level in guts of Hinfp- or His1-rescued flies (Fig. 6 *F*–*I*). Whole-genome RNAseq analysis of guts revealed that transgenic expression of either Hinfp or His1 was sufficient to resume repression of most TEs (Fig. 6*J* and *SI Appendix*, Fig. S6 *A*–*C*) and further confirmed by qPCR of many TEs using gut RNA (Fig. 6*K*). More than half of the misregulated *Drosophila* genes, particularly those that showed derepression (Fig. 6*L*, red color in *Hinfp*^{2} mutant lane), were also rescued by the expression of Hinfp or His1.

We also examined the connection between mobilization of TEs and genome damage in the *Hinfp* mutants. Many TEs in *Drosophila* are retrotransposable elements, and some reverse-transcriptase inhibitors used for antiviral treatment in humans have been shown to be effective in inhibiting TE-induced genome damage and aging phenotypes in *Drosophila* (55–57). We therefore added the inhibitors Zidovudine (azidothymidine, AZT) and Lamivudine (dideoxy-3-thiacytidine, 3TC) in the fly food for feeding during embryonic–larval–pupal development. There was reduction of γH2Av staining, most obviously in posterior midguts of *Hinfp* mutant pupae (*SI Appendix*, Fig. S7). Interestingly, some γH2Av staining was still present in precursor cells (*SI Appendix*, Fig. S7*C*, arrows), while ECs showed almost no staining. This suggests that ECs that have absorptive function may be able to retain higher levels of the inhibitors to suppress more efficiently the TE-induced DNA damage. Together, the results demonstrate that the Hinfp–His1 axis is responsible for repression of most TEs, as well as many *Drosophila* genes, in somatic tissues to maintain genome integrity.

Loss of Hinfp Promotes Aging- and Cancer-Related Phenotypes. Genome instability and abnormal TE activity can lead to many pathological consequences (3, 6, 9–11, 25, 58). To examine whether loss of Hinfp might have such outcomes, we examined the functional requirement of Hinfp in neurons during aging (*SI Appendix*, Fig. S8). The elav–Gal4 drives the expression in all developing and adult neurons. The development of animals containing elav–Gal4-driven *Hinfp* dsRNA raised at 23 °C appeared normal and eclosed as adult flies. However, the aging flies had significantly shorter life spans (*SI Appendix*, Fig. S8*A*). Furthermore, younger flies at around 20 d old that still had rather normal viability nonetheless showed highly declined climbing ability (*SI Appendix*, Fig. S8 *B*–*D*), similar to other cases of motor neuron defects (59).

We also crossed a UAS–dsRNA construct of *Hinfp* together with an oncogenic construct, UAS–Ras^{V12}. Ras^{V12} is a widely used gain-of-function mutation that induces cell growth and polarity abnormalities in multiple *Drosophila* tissues, resembling many cancer-related phenotypes in humans (60–64). We used the esg^{ts}> as the driver and performed the experiments at the ambient temperature of 23 °C to allow moderate expression of the transgenes throughout development. The *esg* driver is expressed in other developing tissues in addition to the aforementioned adult midgut ISCs/EBs. By following the UAS–GFP marker expression, we found that the normally proliferative midgut precursor cells in the third-instar larvae exhibited substantially increased cell number (top of *SI Appendix*, Fig. S9 *A*–*H*), resembling tumor clusters after coexpression of *Hinfp* dsRNA and Ras^{V12} when compared to each transgene alone (two sets of images in *SI Appendix*, Fig. S9 *A*–*H*). Moreover, the larval salivary glands normally contain differentiated cells, but the coexpression of *Hinfp* dsRNA and Ras^{V12} caused a highly twisted morphology of the glands, indicative of further cellular transformation when compared to expression of either construct alone (*SI Appendix*, Fig. S9 *I*–*L*). The coexpression of *Hinfp* dsRNA and Ras^{V12} also resulted in fewer eclosed adult flies, demonstrating a synthetic lethality (*SI Appendix*, Fig. S9*M*). These results together illustrate that loss of Hinfp can exacerbate cancer- and aging-related phenotypes, but whether this is caused by genome instability or other mechanisms requires further investigation.

We have examined the expression of various Histones using the human 293 cell line after knockdown of HINFP (*SI Appendix*, Fig. S9*N*). We found that not only His4 expression was decreased, as previously described, but two variants of His1, namely, His1.X and His1.O, were also decreased, while overall His1 expression revealed by a pan-His1 antibody exhibited no significant change. The LINE-1 TE family has over 70,000 copies and is the major active element in the human genome (4). An antibody recognizing the product of open reading frame 2 of LINE-1 revealed an increase of overall expression after HINFP RNAi. Therefore, these expression analyses provide evidence that Hinfp regulation of His1 and TEs may be evolutionarily conserved.

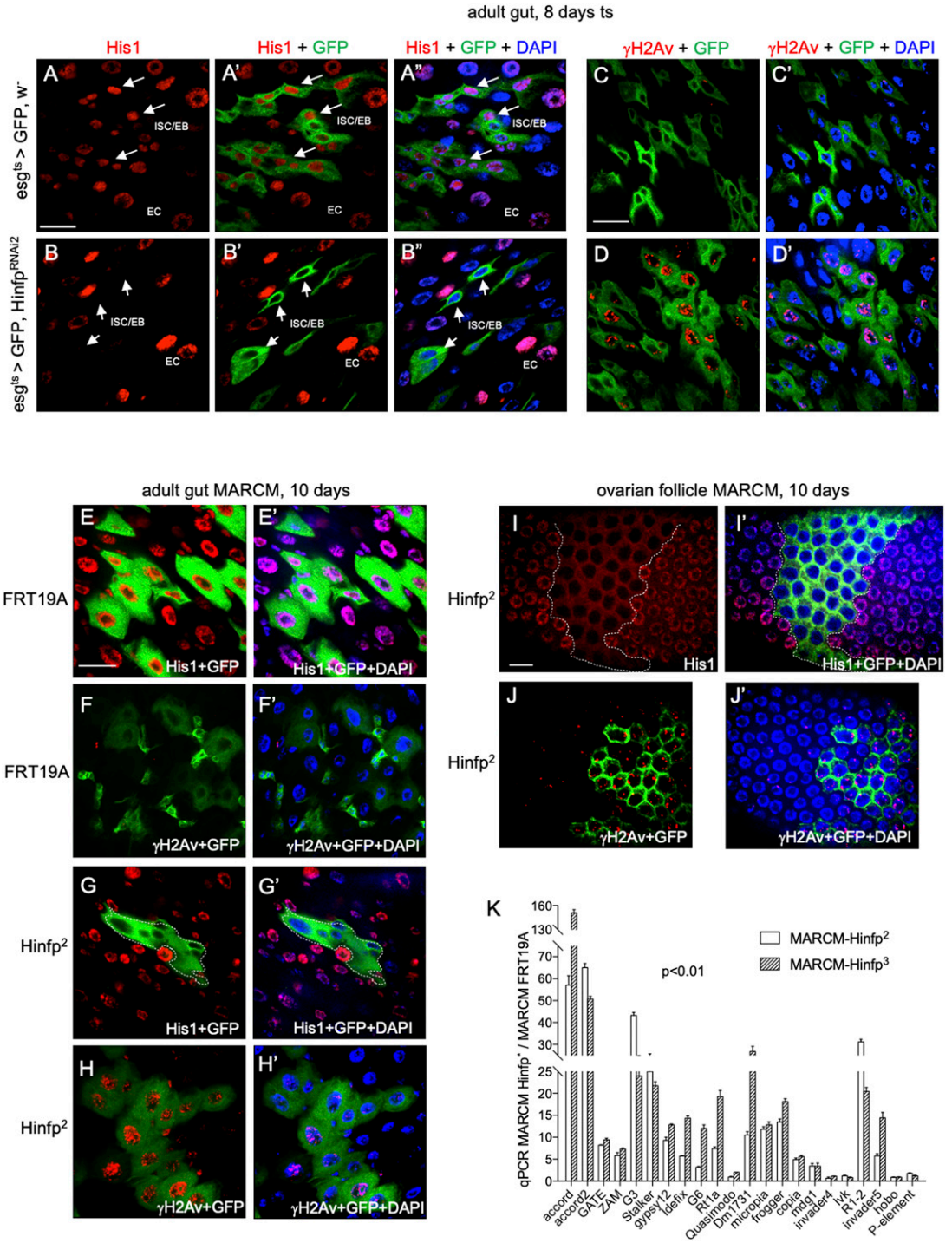

Fig. 5. Regulation of His1 expression, TE repression, and genome integrity by Hinfp is cell-autonomous. (*A*–*D*) Confocal images of midguts from adult offspring from crosses of *escargot* promoter–Gal4, UAS–mCD8GFP; tubulin–Gal80^{ts} (esg^{ts} > GFP) with w^{1118} control or with UAS–Hinfp–dsRNA (Hinfp^{RNAi}). The eclosed offspring were grown for 5 to 7 d and then incubated at 29 °C for 8 d to induce RNAi. Guts were dissected from female flies and used for immunostaining and microscopy. The esg^{ts} > GFP driver marked the ISC/EB precursor cells (three of them are indicated by arrows), while the bigger ECs did not have GFP. After *Hinfp* RNAi, the GFP-labeled precursor cells lost their His1 staining (*B*) and had increased γH2Av staining (*D*) in their nuclei. (Scale bars: 20 μm.) (*E*–*J*) Confocal images of midgut and ovarian follicle epithelia from MARCM adult female flies. Homozygous $Hinfp^{-/-}$ clones positively marked by GFP were induced by heat-shock-controlled expression of the FLP recombinase and let grow for 10 d. Guts and ovaries were dissected and stained for His1 and γH2Av. The FRT19A control clones (*E*, *F*, and *I*), as well as GFP^{-} cells surrounding $Hinfp^{-/-}$ mutant clones, had clear nuclear His1 staining and very low γH2Av staining. The GFP+ mutant clones, also outlined by white dashed lines in *G* and *I*, showed loss of His1. Similar mutant clones showed increased γH2Av staining (*H* and *J*). (Scale bars: 20 μm.) (*K*) RNA expression of TEs in guts containing MARCM clones by qPCR. Flies were heat-shocked multiple times to induce more clones and let recover for 10 d, and 30 guts from female flies were dissected and used for RNA isolation and qPCR. Each qPCR experiment included the *rp49* PCR in parallel as internal control, and the expression of each TE in control FRT19A was set as one. The expression levels in guts containing mutant clones were plotted as fold increase over the levels in guts containing FRT19A wild-type clones. The average is from three independent experiments, with SEM as error bar, and most TEs had a significant increase, with $P < 0.01$.

A Hinfp*/FM7c ; tubGal4/TM6B X w-/Y ; +/+
X w/Y ; UAS-HA-transgene

Genotype of *Hinfp*- offspring	Number of *Hinfp*- male/total male
Hinfp^2/Y ; tubGal4/+	4.9% (6/122)
Hinfp^3/Y ; tubGal4/+	2.7% (3/111)
Hinfp^2/Y ; tubGal4/UAS-Hinfp	63.4% (92/145)
Hinfp^3/Y ; tubGal4/UAS-Hinfp	73.4% (69/94)
Hinfp^2/Y ; tubGal4/UAS-His1	54.2% (180/332)
Hinfp^3/Y ; tubGal4/UAS-His1	57.0% (155/272)
Hinfp^2/Y ; tubGal4/UAS-His4	2.6% (1/39)
Hinfp^3/Y ; tubGal4/UAS-His4	0% (0/45)
Hinfp^2/Y ; tubGal4/UAS-msn	2.0% (1/51)
Hinfp^3/Y ; tubGal4/UAS-msn	0% (0/47)

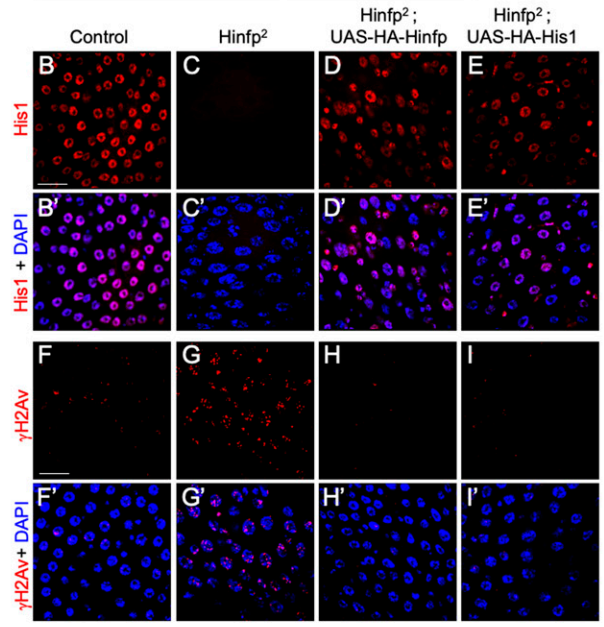

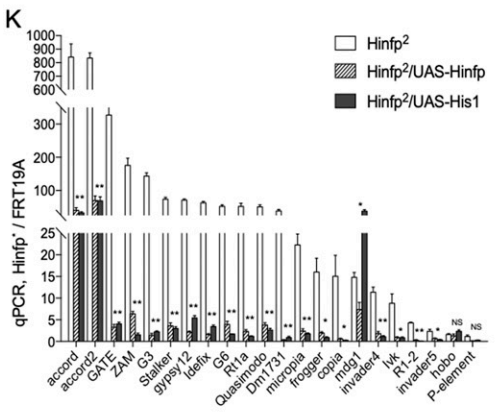

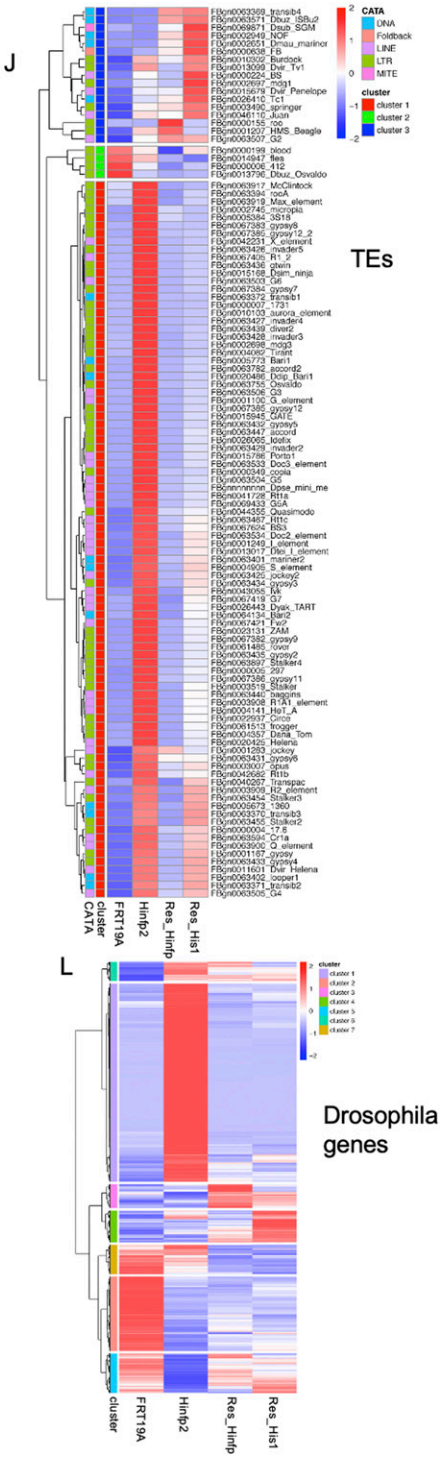

Fig. 6. His1 functions downstream of Hinfp to repress TEs and maintain genome integrity. (*A*) Quantification of viable flies in the presence of UAS–*Hinfp*, –*His1*, –*His4*, or –*msn* cDNA transgenes. These transgenes were each crossed with the two *Hinfp* mutants and the tubulin–Gal4 ubiquitous driver. Adult male flies that contained the correct chromosomes based on the absence of balancer markers were counted. The percentage and total number of flies in parentheses, obtained from four independent crosses, are shown. (*B–I*) Confocal images after staining for His1 or γH2Av in midguts of newly eclosed adults or mutant pharate adults. (Scale bars: 20 μm.) (*J*) Heatmap of TE expression based on RNAseq of gut samples from control, *Hinfp*^{2} mutant pharate, or rescued male adults. The expression of each TE in the four samples were calculated as a Z-score from low/blue (–2) to high/red (+2). (*K*) Quantification of TE expression by qPCR of gut RNA from FRT19A control, mutant or rescued animals. The expression level was compared to *rp49* for each sample and set as one for each TE in control flies, and the expression in other samples was plotted as fold change. The results represent the average of three independent experiments, and error bars represent SEM. $^{**}P < 0.01$. $^{*}P < 0.05$. NS, not significant. (*L*) Heatmap of expression of significantly differentially expressed *Drosophila* genes in the *Hinfp*^{2} mutant and rescued RNAseq dataset. The relative expression of each sequence in the control, mutant and rescued samples was calculated as a Z-score and shown as low/blue (–2) to high/red (+2). A large portion of the genes that are up-regulated in the mutant (cluster 1, upper half of heat map, red in *Hinfp*^{2}) changed back to similar to the control FRT19A in the presence of either the *Hinfp* or *His1* transgene (blue in control and rescued).

Discussion

In this report, we establish a previously unknown function of *Drosophila* Hinfp that is to safeguard somatic genomes by maintaining repression of most TEs, as well as many *Drosophila* genes (*SI Appendix*, Fig. S9*O*). By examining multiple tissues, cell-specific RNAi, clonal analysis, and genetic rescue, we show that a key target gene of Hinfp in this process is *His1*. His1 functions as linker histones required for higher-order chromatin assembly. *His1* expression, but not *His4* expression, is sufficient to rescue most of the *Hinfp* mutant phenotypes. With the derepression of most TEs in the mutants, our results suggest that this Hinfp–His1 axis represents a key TE silencing mechanism in somatic tissues. Nonetheless, this Hinfp–His1 axis also up- or down-regulates over 1,000 *Drosophila* genes in both euchromatic and heterochromatic regions (Fig. 2 and *SI Appendix*, Table S2; https://doi.org/10.6084/m9.figshare.15506415.v1) that may play a role in genome stability (*SI Appendix*, Fig. S9*O*). Moreover, the observed increase in γH2Av could be due to TE mobility, as well as mobility-unrelated transcriptional up-regulation of TE loci, such as R-loop formation at TE loci upon transcriptional up-regulation, as proposed by a previous model (48).

Mammalian HINFP has been well known for regulating His4 expression to provide an appropriate amount of His4 for core nucleosome assembly during DNA replication (34–37). His1 serves as the linker histone required for higher-order chromatin assembly, which allows more efficient gene silencing, either as local compact chromatin or as large regions of heterochromatin, such as those around centromere or telomere (7, 47). Loss of His1 in mammals and *Drosophila* leads to both global and locus-specific phenotypes (43–51). *Drosophila Histone* genes are arranged in the order of *His1*, *His2A*, *His2B*, *His4*, and *His3*, repeated 23 times. While the expression of core histone genes is coordinated with the cell cycle, the regulation of *His1* genes in *Drosophila* is not cell-cycle-dependent. This unique regulation of the *Drosophila His1* gene is partly dependent on promoter sequences and the TATA-related factor TRF2 (42, 65), which also regulates piRNA and TEs in germline (16, 22, 66). Interestingly, our human 293 cells results also point to the regulation by HINFP of His1.X and His1.O, which are non-cell-cycle-dependent variants (47, 67, 68). Meanwhile, most other mammalian His1 are cell-cycle-dependent variants, and they do not seem to be affected after knockdown of HINFP based on our Western blots. A previous report by whole-genome chromatin immunoprecipitation and sequencing assays in mammalian cells shows that HINFP binding peaks are detected on *His1.X* and *His1.O* genomic loci, but not other *His1* genes (69). Therefore, we propose that Hinfp regulation of cell-cycle-independent His1 variants is a conserved mechanism to repress TEs in somatic tissues.

Even in germ cells, chromatin structure plays an important role in collaborating with the well-studied piRNA pathway, therefore combining the efficiency of transcriptional and posttranscriptional silencing of TEs (14, 15, 22, 25, 70). Because the piRNA and siRNA pathways appear to play a minor role in somatic cells to repress TEs, heterochromatin formation and its regulation may become a key mechanism in somatic tissues. Previous studies show that knockdown of *His1* expression by RNAi in *Drosophila* and mammalian somatic cells results in various chromatin defects and derepression of TEs (43–51). It is remarkable that over 60% of TEs, but less than 10% of *Drosophila* host genes, are derepressed in *His1* RNAi or in *Hinfp* mutants. Our rescue experiments clearly demonstrate that Hinfp as a single zygotic gene product acts as a pivotal physiological regulator of this His1-dependent silencing of most TEs, therefore providing a venue to study this process in somatic genomes.

The loss of regulation of somatic TEs has long been proposed to impact progression of many diseases (3, 4, 7, 10, 12). We show that the loss of Hinfp in the nervous system causes premature aging that may be related to neurodegeneration. Furthermore, our genetic interaction experiment of loss of Hinfp with oncogenic Ras demonstrates multiple pathological consequences, including abnormal proliferation and tissue transformation. However, genetic interaction experiments have caveats, and the overgrowth of the larval midgut precursor clusters can come from different possibilities, which may or may not be due to the loss of Histone1 or genome damage after complete loss of function of Hinfp, such as misregulation of other genes that instead cooperate with RasV12. It is also possible that there is a low level of H1 reduction and genome damage, but it is sufficient to activate a yet-to-be-identified pathway that cooperates with activated RasV12 to increase growth. Further investigation is required to understand the underlying mechanism that mediates this growth enhancement. Overall, our results suggest that Hinfp may serve as an important target to study cancer progression, neurodegeneration, and aging that are affected by higher-order chromatin structure, TE silencing, and genome stability.

Materials and Methods

Detailed methods and materials, including *Drosophila* stocks and transgenic lines; generation of *Hinfp* mutants by CRISPR/Cas9-mediated genome editing; genetic mosaic analysis by MARCM; transgenic rescue and feeding rescue experiments; RNA preparation and real-time qPCR; immunostaining; antibodies and microscopy; extraction and immunoblot protein analysis; genomic DNA extraction and native agarose gel analysis; RNA deep sequencing and analysis; and statistical analysis are listed in *SI Appendix*.

Data Availability. All study data are included in the article and/or *SI Appendix*. Data are original and have been deposited in the GEO database (GEO accession no. GSE138430) (71), and supplementary Tables 1 and 2 for Histone and heterochromatic gene expression dataset Excel tables are available in FigShare (https://doi.org/10.6084/m9.figshare.15506415.v1) (72).

ACKNOWLEDGMENTS. We thank W. Theurkauf for help with TE analysis. Stocks obtained from the Bloomington Drosophila Stock Center (NIH Grant P40OD018537) were used in this study. We also acknowledge the Vienna *Drosophila* Research Center and Drosophila Genomics Resource Center for transgenic lines. Y.T.I. was supported by NIH Grants DK083450 and GM107457. Y.T.I. is a member of the UMass Center for Clinical and Translational Science (NIH Grant UL1TR000161).

1. D. Haig, Transposable elements: Self-seekers of the germline, team-players of the soma. *BioEssays* **38**, 1158–1166 (2016).
2. S. M. Gasser, Selfish DNA and epigenetic repression revisited. *Genetics* **204**, 837–839 (2016).
3. K. H. Burns, Our conflict with transposable elements and its implications for human disease. *Annu. Rev. Pathol.* **15**, 51–70 (2020).
4. R. N. Platt 2nd, M. W. Vandewege, D. A. Ray, Mammalian transposable elements and their impacts on genome evolution. *Chromosome Res.* **26**, 25–43 (2018).
5. P. A. Larsen, Transposable elements and the multidimensional genome. *Chromosome Res.* **26**, 1–3 (2018).
6. J. X. Feng, N. C. Riddle, Epigenetics and genome stability. *Mamm. Genome* **31**, 181–195 (2020).
7. S. J. Klein, R. J. O'Neill, Transposable elements: Genome innovation, chromosome diversity, and centromere conflict. *Chromosome Res.* **26**, 5–23 (2018).
8. P. Rojas-Ríos, M. Simonelig, piRNAs and PIWI proteins: Regulators of gene expression in development and stem cells. *Development* **145**, dev161786 (2018).
9. Y. H. Chang, J. Dubnau, The gypsy endogenous retrovirus drives non-cell-autonomous propagation in a *Drosophila* TDP-43 model of neurodegeneration. *Curr. Biol.* **29**, 3135–3152.e4 (2019).
10. C. Guo *et al.*, Tau activates transposable elements in Alzheimer's disease. *Cell Rep.* **23**, 2874–2880 (2018).
11. G. D. Guler *et al.*, Repression of stress-induced LINE-1 expression protects cancer cell subpopulations from lethal drug exposure. *Cancer Cell* **32**, 221–237.e13 (2017).
12. K. Siudeja *et al.*, Unraveling the features of somatic transposition in the *Drosophila* intestine. *EMBO J.* **40**, e106388 (2021).
13. R. J. Ross, M. M. Weiner, H. Lin, PIWI proteins and PIWI-interacting RNAs in the soma. *Nature* **505**, 353–359 (2014).
14. K. Sato, M. C. Siomi, The piRNA pathway in *Drosophila* ovarian germ and somatic cells. *Proc. Jpn. Acad., Ser. B, Phys. Biol. Sci.* **96**, 32–42 (2020).
15. D. M. Ozata, I. Gainetdinov, A. Zoch, D. O'Carroll, P. D. Zamore, PIWI-interacting RNAs: Small RNAs with big functions. *Nat. Rev. Genet.* **20**, 89–108 (2019).

16. S. S. Parhad *et al*., Adaptive evolution targets a piRNA precursor transcription network. *Cell Rep.* **30**, 2672–2685.e5 (2020).
17. M. van den Beek *et al*., Dual-layer transposon repression in heads of *Drosophila melanogaster*. *RNA* **24**, 1749–1760 (2018).
18. B. Barckmann *et al*., The somatic piRNA pathway controls germline transposition over generations. *Nucleic Acids Res.* **46**, 9524–9536 (2018).
19. P. Sousa-Victor *et al*., Piwi is required to limit exhaustion of aging somatic stem cells. *Cell Rep.* **20**, 2527–2537 (2017).
20. B. C. Jones *et al*., A somatic piRNA pathway in the *Drosophila* fat body ensures metabolic homeostasis and normal lifespan. *Nat. Commun.* **7**, 13856 (2016).
21. M. Ghildiyal *et al*., Endogenous siRNAs derived from transposons and mRNAs in *Drosophila* somatic cells. *Science* **320**, 1077–1081 (2008).
22. P. R. Andersen, L. Tirian, M. Vunjak, J. Brennecke, A heterochromatin-dependent transcription machinery drives piRNA expression. *Nature* **549**, 54–59 (2017).
23. J. G. Wood *et al*., Chromatin-modifying genetic interventions suppress age-associated transposable element activation and extend life span in *Drosophila*. *Proc. Natl. Acad. Sci. U.S.A.* **113**, 11277–11282 (2016).
24. S. Porazinski *et al*., EphA2 drives the segregation of ras-transformed epithelial cells from normal neighbors. *Curr. Biol.* **26**, 3220–3229 (2016).
25. C. A. Ishak *et al*., An RB-EZH2 complex mediates silencing of repetitive DNA sequences. *Mol. Cell* **64**, 1074–1087 (2016).
26. J. C. Yasuhara, B. T. Wakimoto, Molecular landscape of modified histones in *Drosophila* heterochromatic genes and euchromatin-heterochromatin transition zones. *PLoS Genet.* **4**, e16 (2008).
27. S. C. Elgin, Heterochromatin and gene regulation in *Drosophila*. *Curr. Opin. Genet. Dev.* **6**, 193–202 (1996).
28. P. Dimitri, Constitutive heterochromatin and transposable elements in *Drosophila melanogaster*. *Genetica* **100**, 85–93 (1997).
29. M. F. Sentmanat, S. C. Elgin, Ectopic assembly of heterochromatin in *Drosophila melanogaster* triggered by transposable elements. *Proc. Natl. Acad. Sci. U.S.A.* **109**, 14104–14109 (2012).
30. B. Ohlstein, A. Spradling, The adult *Drosophila* posterior midgut is maintained by pluripotent stem cells. *Nature* **439**, 470–474 (2006).
31. C. A. Micchelli, N. Perrimon, Evidence that stem cells reside in the adult *Drosophila* midgut epithelium. *Nature* **439**, 475–479 (2006).
32. L. Gervais, A. J. Bardin, Tissue homeostasis and aging: New insight from the fly intestine. *Curr. Opin. Cell Biol.* **48**, 97–105 (2017).
33. R. K. Zwick, B. Ohlstein, O. D. Klein, Intestinal renewal across the animal kingdom: Comparing stem cell activity in mouse and *Drosophila*. *Am. J. Physiol. Gastrointest. Liver Physiol.* **316**, G313–G322 (2019).
34. P. N. Ghule *et al*., Higher order genomic organization and regulatory compartmentalization for cell cycle control at the G1/S-phase transition. *J. Cell. Physiol.* **233**, 6406–6413 (2018).
35. R. Medina *et al*., The histone gene cell cycle regulator HiNF-P is a unique zinc finger transcription factor with a novel conserved auxiliary DNA-binding motif. *Biochemistry* **47**, 11415–11423 (2008).
36. R. Xie *et al*., The histone gene activator HINFP is a nonredundant cyclin E/CDK2 effector during early embryonic cell cycles. *Proc. Natl. Acad. Sci. U.S.A.* **106**, 12359–12364 (2009).
37. L. J. Liu *et al*., Functional coupling of transcription factor HiNF-P and histone H4 gene expression during pre- and post-natal mouse development. *Gene* **483**, 1–10 (2011).
38. S. Yamamoto *et al*., A *Drosophila* genetic resource of mutants to study mechanisms underlying human genetic diseases. *Cell* **159**, 200–214 (2014).
39. N. Ozawa *et al*., Organ identity specification factor WGE localizes to the histone locus body and regulates histone expression to ensure genomic stability in *Drosophila*. *Genes Cells* **21**, 442–456 (2016).
40. W. Zhang *et al*., Probing the function of metazoan histones with a systematic library of H3 and H4 mutants. *Dev. Cell* **48**, 406–419.e5 (2019).
41. D. J. McKay *et al*., Interrogating the function of metazoan histones using engineered gene clusters. *Dev. Cell* **32**, 373–386 (2015).
42. B. Guglielmi, N. La Rochelle, R. Tjian, Gene-specific transcriptional mechanisms at the histone gene cluster revealed by single-cell imaging. *Mol. Cell* **51**, 480–492 (2013).
43. N. Yusufova *et al*., Histone H1 loss drives lymphoma by disrupting 3D chromatin architecture. *Nature* **589**, 299–305 (2021).
44. G. Sollberger *et al*., Linker histone H1.2 and H1.4 affect the neutrophil lineage determination. *eLife* **9**, e52563 (2020).
45. Y. Fan *et al*., Histone H1 depletion in mammals alters global chromatin structure but causes specific changes in gene regulation. *Cell* **123**, 1199–1212 (2005).
46. K. Cao *et al*., High-resolution mapping of h1 linker histone variants in embryonic stem cells. *PLoS Genet.* **9**, e1003417 (2013).
47. S. E. Healton *et al*., H1 linker histones silence repetitive elements by promoting both histone H3K9 methylation and chromatin compaction. *Proc. Natl. Acad. Sci. U.S.A.* **117**, 14251–14258 (2020).
48. A. Bayona-Feliu, A. Casas-Lamesa, O. Reina, J. Bernués, F. Azorín, Linker histone H1 prevents R-loop accumulation and genome instability in heterochromatin. *Nat. Commun.* **8**, 283 (2017).
49. E. N. Andreyeva *et al*., Regulatory functions and chromatin loading dynamics of linker histone H1 during endoreplication in *Drosophila*. *Genes Dev.* **31**, 603–616 (2017).
50. X. Lu *et al*., *Drosophila* H1 regulates the genetic activity of heterochromatin by recruitment of Su(var)3-9. *Science* **340**, 78–81 (2013).
51. O. Vujatovic *et al*., *Drosophila melanogaster* linker histone dH1 is required for transposon silencing and to preserve genome integrity. *Nucleic Acids Res.* **40**, 5402–5414 (2012).
52. Q. Li *et al*., The conserved misshapen-warts-Yorkie pathway acts in enteroblasts to regulate intestinal stem cells in *Drosophila*. *Dev. Cell* **31**, 291–304 (2014).
53. A. Amcheslavsky, J. Jiang, Y. T. Ip, Tissue damage-induced intestinal stem cell division in *Drosophila*. *Cell Stem Cell* **4**, 49–61 (2009).
54. T. Lee, L. Luo, Mosaic analysis with a repressible cell marker (MARCM) for *Drosophila* neural development. *Trends Neurosci.* **24**, 251–254 (2001).
55. B. Goic *et al*., RNA-mediated interference and reverse transcription control the persistence of RNA viruses in the insect model *Drosophila*. *Nat. Immunol.* **14**, 396–403 (2013).
56. L. Krug *et al*., Retrotransposon activation contributes to neurodegeneration in a *Drosophila* TDP-43 model of ALS. *PLoS Genet.* **13**, e1006635 (2017).
57. A. M. Casale *et al*., Transposable element activation promotes neurodegeneration in a *Drosophila* model of Huntington's disease. *bioRxiv* [Preprint] (2020). https://doi.org/10.1101/2020.11.19.389718 (Accessed 19 November 2020).
58. W. Li *et al*., Human endogenous retrovirus-K contributes to motor neuron disease. *Sci. Transl. Med.* **7**, 307ra153 (2015).
59. Y. Yuva-Aydemir, S. Almeida, G. Krishnan, T. F. Gendron, F. B. Gao, Transcription elongation factor AFF2/FMR2 regulates expression of expanded GGGGCC repeat-containing C9ORF72 allele in ALS/FTD. *Nat. Commun.* **10**, 5466 (2019).
60. Y. Nie *et al*., Oncogenic pathways and loss of the Rab11 GTPase synergize to alter metabolism in *Drosophila*. *Genetics* **212**, 1227–1239 (2019).
61. L. Murcia, M. Clemente-Ruiz, P. Pierre-Elies, A. Royou, M. Milán, Selective killing of RAS-malignant tissues by exploiting oncogene-induced DNA damage. *Cell Rep.* **28**, 119–131.e4 (2019).
62. B. S. Dunn, L. Rush, J. Y. Lu, T. Xu, Mutations in the *Drosophila* tricellular junction protein M6 synergize with Ras^{V12} to induce apical cell delamination and invasion. *Proc. Natl. Acad. Sci. U.S.A.* **115**, 8358–8363 (2018).
63. J. B. Cordero *et al*., Oncogenic Ras diverts a host TNF tumor suppressor activity into tumor promoter. *Dev. Cell* **18**, 999–1011 (2010).
64. J. Lee, A. J. H. Cabrera, C. M. T. Nguyen, Y. V. Kwon, Dissemination of Ras^{V12}-transformed cells requires the mechanosensitive channel Piezo. *Nat. Commun.* **11**, 3568 (2020).
65. Y. Isogai, S. Keles, M. Prestel, A. Hochheimer, R. Tjian, Transcription of histone gene cluster by differential core-promoter factors. *Genes Dev.* **21**, 2936–2949 (2007).
66. I. S. Osadchiy, P. G. Georgiev, O. G. Maksimenko, Functional comparison of short and long isoforms of the TRF2 protein in *Drosophila melanogaster*. *Dokl. Biochem. Biophys.* **486**, 224–228 (2019).
67. C. M. Di Liegro, G. Schiera, I. Di Liegro, H1.0 linker histone as an epigenetic regulator of cell proliferation and differentiation. *Genes (Basel)* **9**, 310 (2018).
68. C. M. Torres *et al*., The linker histone H1.0 generates epigenetic and functional intratumor heterogeneity. *Science* **353**, aaf1644 (2016).
69. M. Sokolova *et al*., Genome-wide screen of cell-cycle regulators in normal and tumor cells identifies a differential response to nucleosome depletion. *Cell Cycle* **16**, 189–199 (2017).
70. Y. W. Iwasaki *et al*., Piwi modulates chromatin accessibility by regulating multiple factors including histone H1 to repress transposons. *Mol. Cell* **63**, 408–419 (2016).
71. N. K. Nirala and Y. Y. Ip, Global transcriptomic analysis of Drosophila Hinfp mutant and wild-type gut to understand their role in genome stability. RNA sequencing fasq data set. https://www.ncbi.nlm.nih.gov/search/all/?term=GSE138430. Deposited 4 October 2019.
72. N. K. Nirala and Y. Y. Ip, Gene expression profile excel for Histone genes and heterochromatic genes in Hinfp mutants. https://figshare.com/articles/dataset/Hinfp_is_a_guardian_of_somatic_genomes_by_repressing_transposable_elements/15506415/1. Deposited 19 August 2021.